Specificity of Soluble Phospholipid Binding Sites on Human Factor X_a†

Mou Banerjee,‡,§ Daryl C. Drummond,§,|| Arvind Srivastava,‡ David Daleke,|| and Barry R. Lentz*,‡

Department of Biochemistry & Biophysics, University of North Carolina at Chapel Hill, Chapel Hill, North Carolina 27599-7260, and Department of Biochemistry & Molecular Biology, Indiana University, Bloomington, Indiana 47405

Received January 8, 2002; Revised Manuscript Received April 10, 2002

ABSTRACT: We explore here the specificities of lipid regulatory sites on factor X_a that affect the rate of factor X_a-catalyzed prothrombin activation. We examined a series of 11 phosphatidylserine (PS) analogues in order to map the structural features of a lipid molecule that are needed to elicit both the structural response and the full increase in activity that can be obtained with the PS molecule. Our observations are interpreted in terms of a model in which factor X_a is regulated by sequential occupancy of a pair of linked lipid binding sites, each of which have different minimum ligand structural requirements to induce structural changes. The first site is apparently of higher affinity and recognizes diacylglycerol (DAG) as a minimal binding structure. The second site is occupied with an affinity slightly less than the first site only when the first is occupied, but binds PS with very low affinity otherwise. It recognizes glycerophosphorylserine (GPS) as the minimal ligand. To test this interpretation, experiments were performed in which more than one lipid species was present. It was necessary to invoke the existence of factor X_a species containing different lipids at each site, each having different structural and functional responses. For optimal activity enhancement, both binding sites must be occupied, the first by PS, although the second can be occupied with other lipids.

During blood coagulation, the zymogen prothrombin is activated to thrombin, the central enzyme of the homeostatic process. This proteolytic activation is catalyzed by an enzyme/cofactor complex (factor X_a/factor V_a) that assembles on membranous vesicles released from activated platelets (*5*, *22*, *23*). Release of platelet vesicles is associated with transbilayer migration of up to 50% of the phosphatidylserine (PS[1]) initially located in the cytoplasmic leaflet of resting platelets (*3*, *4*). It appears that the appearance of acidic phospholipids, specifically PS, on the surface of these platelet-derived vesicles is essential for the assembly of an active prothrombinase (*9*, *16*, *19*, *23*).

We have shown that a soluble form of PS (C6PS[1]) enhanced the rate of prothrombin activation by factor X_a by 60-fold (*18*). More recently, we have observed that binding of this soluble form of PS elicited conformational changes in factor X_a, as judged by an active-site-located fluorescent probe, secondary structure, and changes in aggregation state in solution (*25*). The simplest interpretation consistent with the various effects of C_6PS on factor X_a was in terms of two, sequentially occupied sites, the first of which was mainly responsible for regulating activity (*25*). The two-site model was confirmed by a series of equilibrium dialysis and CD experiments on fragments or multiple-domains of factor X_a (*24*). The site that regulates activity is in the N-terminal portion of factor X_a (probably in the EGF domains or in the Gla domain when covalently attached to the EGF domains), while the second site is an anomalous site in the catalytic domain and is actually part of the substrate recognition site (*24*). These studies have suggested that occupancy of the second site is altered by occupancy of the regulatory site, although direct demonstration of this by ligand competition or cooperation studies has been lacking.

Soluble phosphatidylglycerol (PG[1]) and phosphatidylcholine (PC[1]) also interacted with factor X_a, but they induced different conformational changes than did soluble PS and did not alter the ability of factor X_a to activate prothrombin (*18*, *25*). Because only C_6PS increased the proteolytic activity

† Supported by USPHS Grants HL45916 to B.R.L. and AM47230 to D.D., and by an American Heart Association Grant-in-Aid to D.D.

* To whom correspondence should be addressed. Tel: (919) 966 5384; Fax: (919) 966 2852; Email: uncbrl@med.unc.edu.

‡ University of North Carolina at Chapel Hill.

§ The first two authors contributed equally to this work.

|| Indiana University.

[1] Abbreviations: ANS, 8-anilino-1-naphthalenesulfonic acid; CMC, critical micelle concentration; C6PS, 1,2-dicaproyl-*sn*-glycero-3-phospho-L-serine; C6PG, 1,2-dicaproyl-*sn*-glycero-3-phospho-*rac*-1-glycerol; C6PC, 1,2-dicaproyl-*sn*-glycero-3-phosphocholine; C6PA, 1,2-dicaproyl-*sn*-glycero-3-phosphate; C6lysoPS, 1-caproyl-2-hydroxy-*sn*-glycero-3-phospho-L-serine; C6lysoPC, 1-caproyl-2-hydroxy-*sn*-glycero-3-phosphocholine; C6lysoPA, 1-caproyl-2-hydroxy-*sn*-glycero-3-phosphate; C6P(D)S, 1,2-dicaproyl-*sn*-glycero-3-phospho-D-serine; C6P(homo)S, 1,2-dicaproyl-*sn*-glycero-3-phospho-D-homoserine; C6P(N-Me)S, 1,2-dicaproyl-*sn*-glycero-3-phospho-L-*N*-methylserine; C8DAG, 1,2-dihexanoylglycerol; CM-52, carboxymethyl cellulose cation-exchange resin; DEGR-CK, [5-(dimethylamino)-1-naphthalenesulfonyl]glutamylycyl-arginyl chloromethyl ketone; DEGR-X_a, factor X_a modified with DEGR-CK; EGTA, ethylene glycol bis(*β*-aminoethyl ether)-*N*,*N*,*N*′,*N*′-tetraacetic acid; GPS, L-α-glycerophosphorylserine; DAG, 1,2-diacylglycerol; PG, 1,2-dioleoyl-3-*sn*-phosphatidylglycerol; PS, phosphatidylserine; RVV-X, Russel's viper venom factor X activating protein; S-2765, *N*-α-benzyloxycarbonyl-D-arginyl-L-glycyl-L-arginine-*p*-nitroanilide dihydrochloride (synthetic substrate for factor X_a); S-2238, phenylalanylpipecolylarginine-*p*-nitroaniline (synthetic substrate for thrombin); SDS−PAGE, sodium dodecyl sulfate−polyacrylamide gel electrophoresis; TLC, thin-layer chromatography; Tris, tris(hydroxymethyl)aminomethane.

10.1021/bi020017p CCC: $22.00
Published on Web 05/17/2002

of factor X_a [Koppaka (*18*)], it is of interest to define the exact molecular features of phospholipids that are required for allosteric regulation of factor X_a and whether both sites contribute to this regulation. In this paper, we report the effects of a variety of soluble PS analogues both on factor X_a structure and on the rate of factor X_a-catalyzed prothrombin activation. The PS analogues, whose chemical structures are shown in Figure 1, were chosen to map the structural features of a lipid molecule that are needed to elicit both the structural response and the increase in activity that can be obtained with the PS molecule. The results suggest that some PS analogues bind to two sites, while others to only one. The first site, the higher affinity regulatory site, depends in its response on Ca^{2+} and recognizes diacylglycerol (DAG[1]) as the simplest effective ligand. The second site, the anomalous site in the catalytic domain, requires Ca^{2+} and is occupied at a somewhat lower affinity only when the first site is occupied and recognizes glycerophosphorylserine (GPS[1]) as a minimal ligand.

EXPERIMENTAL PROCEDURES

Materials

Lipid stock suspensions in buffer were prepared fresh for titration experiments by measuring aliquots of appropriate lipid stocks in chloroform, evaporating the chloroform under a stream of nitrogen, resolubilizing the lipid in cyclohexane, and then lyophilizing these frozen solutions overnight. The resulting dry powder was dispersed in the appropriate buffer and vortexed thoroughly. Lipid stock suspensions were generally used without freezing and within 15 h of preparation. 1,2-Dicaproyl-*sn*-glycero-3-phospho-L-serine (C6PS[1]), 1,2-dicaproyl-*sn*-glycero-3-phospho-*rac*-1-glycerol (C6PG[1]), 1,2-dicaproyl-*sn*-glycero-3-phosphocholine (C6PC[1]), 1,2-dicaproyl-*sn*-glycero-3-phosphate (C6PA[1]), 1-caproyl-2-hydroxy-*sn*-glycero-3-phosphocholine (C6lysoPC[1]), and 1-caproyl-2-hydroxy-*sn*-glycero-3-phosphate (C6lysoPA[1]) were purchased from Avanti Polar Lipids (Alabaster, AL). L-Homoserine, D-serine, phospholipase D from *Streptomyces species*, L-serine, *O*-phospho-L-serine, L-α-glycerophosphorylserine (GPS[1]), and phospholipase A_2 from *Naja naja naja* venom were purchased from Sigma Chemical Co. (St. Louis, MO). *N*-Methylserine was purchased from BACHEM Bioscience Inc. (Philadelphia, PA). 1,2-Dioctanoylglycerol (C8DAG[1]) was obtained from Doosan Sedery Research Laboratories (Englewood Cliffs, NJ). Octyl β-glucoside was obtained from Pierce (Rockford, IL). RVV-X[1] activator was purchased from Haematologic Technologies Inc. (Essex Junction, VT). [5-(Dimethylamino)-1-naphthalenesulfonyl]-glutamylcylarginyl chloromethyl ketone (DEGR-CK[1]) was purchased from Calbiochem (La Jolla, CA). *N*-α-Benzyloxycarbonyl-D-arginyl-L-glycyl-L-arginine-*p*-nitroanilide dihydrochloride (S-2765[1]) and phenylalanylpipecolylarginine-*p*-nitroaniline (S-2238[1]) were purchased from Chromogenix (Molndal, Sweden). All other chemicals were ACS reagent grade or the best available grade.

Methods

Analysis of Short-Chain Lipids. The stability of several short-chained phospholipids was examined by thin-layer chromatography upon storage for 1 h at 37 °C, for 24 h at 4 °C, and for several months at −20 °C. The separated products were quantified by phosphate analysis (*2*). Less than 3% hydrolysis of ester linkages to the corresponding lysophospholipid was observed under any of these conditions. Hydrolysis of the phosphate ester was not observed under these conditions.

Critical micelle concentrations (CMC's[1]) of short-chain lipids were determined in the presence of factor X_a by ANS[1] fluorescence, as described previously (*18*). All titration experiments and/or analyses of data were carried below the measured CMC's of short chain C6PS and its analogues. Concentrations of the phospholipid stock solutions were estimated by inorganic phosphate determination (*8*).

Synthesis of Short-Chain Phosphatidylserine Analogues. 1,2-Dicaproyl-*sn*-glycero-3-phospho-D-serine [C6P(D)S[1]], 1,2-dicaproyl-*sn*-glycero-3-phospho-D-homoserine [C6P-(homo)S[1]], 1,2-dicaproyl-*sn*-glycero-3-phosphate (C6PA[1]), and 1,2-dicaproyl-*sn*-glycero-3-phospho-L-*N*-methylserine [C6P(N-Me)S[1]] were synthesized by a phospholipase D catalyzed transphosphatidylation reaction using a one-phase system as described previously (*9*, *10*). Briefly, C6PC was dried under nitrogen and subsequently under vacuum for 2 h to remove any residual solvent. The lipid was resuspended at a final concentration of 75−80 mM in a calcium acetate buffer (100 mM $CaCl_2$, 100 mM acetate, pH 5.6) containing 2% β-octylglucoside and saturating concentrations of the corresponding alcohol; 80% (w/v) *N*-methylserine, 46% D-serine (w/v), 60% L-homoserine (w/v), or buffer for phosphatidic acid. The pH of the buffer was adjusted to pH 5.6 during the solubilization of the alcohol. The reaction mixture was mechanically stirred at 35 °C, and phospholipase D from *Streptomyces species* was added to 15−25 units/mL of reaction mixture. The source of phospholipase D is important, as phospholipase D from other sources such as *Streptomyces chromofuscus* or cabbage results in higher yields of phosphatidic acid and lower yields of the desired transphosphatidylation product (*9*, *17*) (Drummond and Daleke, unpublished observations). The reaction was slowed every 15 min by incubation on ice and the progress of the reaction assayed by normal phase, silica gel, thin-layer chromatography using an acidic solvent system ($CHCl_3$/CH_3-OH/HCOOH, 60:40:5). Reaction was detected using a phosphomolybdenum spray reagent (Sigma Chemical Co., St. Louis, MO) to detect phosphate-containing compounds, a fluorescamine (0.05% w/v in acetone) spray to detect compounds containing a primary amine group, and iodine vapor to detect lipids. An additional aliquot of phospholipase D (again to 15−25 units/mL) was added, and the mixture was reincubated at 35 °C. This procedure was repeated until substrate was no longer detected, and the reaction was stopped by the addition of 100 mM EGTA.

The derivatives were purified by first adding 2.5 volumes of $CHCl_3$ and 1 volume of deionized, distilled water to the reaction mixture and allowing the phases to separate. The β-octylglucoside detergent was found mostly in the cloudy interfacial region and was discarded. The L-homoserine and *N*-methylserine derivatives were found primarily in the aqueous (upper) phase, and the D-serine derivative was found primarily in the organic (lower) phase. The aqueous phase was then dried by azeotropic rotoevaporation following the addition of ethanol. The lipid was resuspended in $CHCl_3$/CH_3OH (1:1), and the precipitated buffer components were

pelleted by centrifugation or removed by filtration. The derivatives finally were purified using CM-52 column chromatography by eluting with increasing concentrations of methanol in chloroform as described (*10*) or by normal silca gel chromatography eluted with $CHCl_3/CH_3OH/HCOOH$ (60:40:5). The identity of purified products was confirmed by ^1H NMR either on a Varian i400 NMR spectrometer operating at 400 MHz or on a Bruker NMR spectrometer operating at 500 MHz and by mass spectroscopy. Dr. Douglas Gage at the NIH Mass Spectrometry Facility collected mass spectra at Michigan State University using negative ion fast atom bombardment (FAB) mass spectrometry with triethanolamine (or glycerol, as noted) used as the matrix. Purified products had the following properties:

(A) sn-1,2-Dicaproylphosphatidylhomoserine [C6P(homo)S]. Conversion (from C6PC): 100%. Mass spectrum (negative ion fast atom bombardment): $m/z = 468$ ($M-H^+$), 490 ($M-H^++Na^+$), and 367 (M−homoserine). ^1H NMR spectrum (500 MHz): δ 4.89 (m, 1H), 4.07 (dd, 1H, $J = 3.0$, 12.0 Hz), 3.83 (dd, 1H, $J = 7.0$, 12.0 Hz), 3.72 (m, 2H), 3.66 (m, 2H), 3.53 (m, 1H), 1.99 (q, 4H, $J = 7.3$ Hz), 1.91 (m, 1H), 1.28 (m, 4H), 0.99 (m, 8H), 0.57 (t, 6H, $J = 6.3$ Hz).

*(B) sn-1,2-Dicaproylphosphatidyl-*D*-serine [C6P(D)S].* Conversion (from dicaproylphosphatidylcholine): 60%. Mass spectrum (negative ion fast atom bombardment): $m/z = 454$ ($M-H^+$), 476 ($M-H^++Na^+$), and 367 (M−serine). ^1H NMR (500 MHz) spectrum: δ 4.90 (m, 1H), 4.09 (dd, 1H, $J = 3.3$, 12.0 Hz), 3.96 (m, 1H), 3.86 (dd, 1H, $J = 6.5$, 12.0 Hz), 3.84 (m, 1H), 3.67 (t, 2H, $J = 5.8$ Hz), 3.43 (m, 1H), 2.00 (q, 4H, $J = 7.6$ Hz), 1.28 (m, 4H), 0.99 (m, 8H), 0.57 (t, 6H, $J = 6.8$ Hz).

(C) sn-1,2-Dicaproylphosphatidyl-N-methylserine [C6P-(N-Me)S]. Conversion (from dicaproylphosphatidylcholine): 32−40%. Mass spectrum (negative ion FAB) showed a peak at $m/z = 468$ ($M-H^+$) and 367 (M−'*N*-methylserine'). ^1H NMR (500 MHz): δ 4.91 (m, 1H), 4.11 (dd, 1H, $J = 3.4$, 12.0 Hz), 4.01 (m, 1H), 3.91 (m, 1H), 3.88 (dd, 1H, $J = 6.5$, 12 Hz), 3.69 (t, 2H, $J = 5.8$ Hz), 3.28 (dd, 1H, $J = 2.9$, 7.0 Hz), 2.44 (s, 3H), 2.02 (q, 4H, $J = 7.4$ Hz), 1.30 (m, 4H), 1.01 (m, 8H), 0.59 (t, 6H, $J = 6.7$ Hz).

(D) sn-1,2-Dicaproylphosphatidic Acid (C6PA). Conversion (from dicaproylphosphatidylcholine): 100%. Mass spectrum (negative ion FAB): $m/z = 367$ ($M-H^+$). ^1H NMR (500 MHz): δ 4.91 (m, 1H), 4.12 (dd, 1H, $J = 3.2$, 12.0 Hz), 3.89 (dd, 1H, $J = 6.7$, 12.0 Hz), 3.66 (m, 2H), 1.99 (q, 4H, $J = 7.3$ Hz), 1.29 (m, 4H), 0.99 (m, 8H), 0.58 (t, $J = 6.7$ Hz).

C6lysoPS[1] and C6lysoPA[1] were synthesized by phospholipase A_2-catalyzed hydrolysis of the ester at the *sn*-2 position for the corresponding dicaproyl phospholipid analogues as described previously (*20*, *21*).

(E) 1-Caproyl-lysophosphatidylserine (C6lysoPS[1]). Conversion from *sn*-1,2-dicaproylphosphatidylserine: 100%. Approximately 1.1 mg of product was isolated following purification. Mass spectra were not obtained due to the low quantity of material isolated. ^1H NMR spectra (400 MHz): δ 3.95 (m, 1H), 2.04 (m, 2H, 8 Hz), 1.30 (m, 2H), 0.57 (t, 3H, $J = 7.0$ Hz). Headgroup and glycerol backbone resonances were not well resolved. The product migrated by TLC with an R_f value equal to 0.16 and was stained with fluorescamine, indicating the presence of a primary amine, and with a phosphomolybdenum spray, indicating the presence of phosphate. Iodine staining revealed only a single spot.

(F) 1-Caproyl-lysophosphatidic acid (C6lysoPA[1]). Conversion from *sn*-1,2-dicaproyl-phosphatidic acid: 100%. Approximately 1.7 mg of product was isolated following purification. Mass spectrum (negative ion FAB, using glycerol as matrix): $m/z = 269$ ($M-H^+$). ^1H NMR spectrum (400 MHz): δ 3.97 (m, 1H), 3.41 (m, 1H), 1.84 (t, 2H, $J = 7.6$ Hz), 1.27 (m, 2H), 0.98 (m, 4H), 0.56 (t, 3H, $J = 6.7$ Hz). Headgroup and glycerol backbone resonances were not well resolved. The product migrated as a single spot by TLC and stained with iodine and phosphomolybdenum spray, indicating the presence of phosphate.

Factor X Isolation. Human factor X was purified from recovered human plasma obtained from The Red Cross according to published methods (*11*, *12*). The factor X obtained in this manner was analyzed by SDS−PAGE[1], concentrated (Centricon-10 concentrator, Amicon Division, W. R. Grace & Co., Danvers, MA), quantitated by UV absorbance at 280 nm using an extinction coefficient of 1.16 mL mg^{-1} cm^{-1} (*13*), and then stored at −70 °C at a concentration of about 1 mg/mL. The day before activation, factor X was purified for the final time by HPLC on a Perkin-Elmer Isopure LC system using a Mono Q HR 5/5 ion exchange column (Pharmacia, Norwalk, CT).

Factor X Activation. Factor X was dialyzed into 50 mM Tris, 0.1 M NaCl, pH 7.5, and activated with a purified fraction of Russel's viper venom factor X activating protein that has been covalently linked to agarose beads (*15*). The activity of factor X_a was measured using the synthetic chromogenic substrate S-2765[1] in an assay adapted to an SLT 340-ATTC microplate reader (Tecan U. S., Hillsborough, NC) according to the method described in Koppaka et al. (*18*).

DEGR-X_a Preparation. DEGR-X_a[1] was prepared by sequential addition of 5 μL of DEGR-CK[1] (1 mg/mL in 0.02 M Tris, 0.1 M NaCl, pH 7.5) to 1 mL of about 17 μM purified factor X_a. The extent of labeling at the active site was followed by the loss of enzymatic activity, as monitored by the S-2765[1] assay. The addition of DEGR-CK was stopped when no activity remained. DEGR-X_a was then dialyzed against 50 mM Tris, 0.1 M NaCl, pH 7.5, to remove free reagent (*14*). DEGR-X_a was analyzed by SDS−PAGE[1] and visualized under UV light with a Foto/Prep II transilluminator (VWR Scientific, Willard, OH).

Fluorescence Titration of DEGR-X_a by Short-Chain Phospholipids. Fluorescence intensity measurements were carried out on an SLM 48000 spectrofluorometer (SLM Aminco, Urbana, IL). Slits were closed between measurements to avoid photodegradation of the sample, and buffer solutions were filtered using 0.2 μm filters (Nalge Co., Rochester, NY). DEGR-X_a (100 nM) in 0.8 mL of buffer (50 mM Tris, 0.1 M NaCl, pH 7.5) was incubated in a stirred micro-cuvette (Hellma Cells, Jamaica, NY) with 5 mM Ca^{2+} at 37 °C for 20 min. Following additions of short-chain phospholipid stocks (1−2 μL each addition for a maximum of 4% dilution), fluorescence intensity was recorded after an equilibration of about 4 min using an excitation wavelength of 340 nm (band-pass 8 nm) and an emission wavelength of 550 nm (band-pass 4 nm). For each addition, several intensity measurements were performed, averaged, and corrected for

the slight decrease in intensity seen for DEGR-X_a in response to titration by buffer only. All binding studies were performed below the CMC of short-chain C6PS and its analogues.

Effect of Short-Chain Phospholipids on Prothrombin Activation. Prothrombin activation was followed using a synthetic substrate (S-2238[1]) to measure thrombin activity. Experimental details of the measurements of the initial rate of prothrombin activation are described elsewhere (*18*). Reaction mixtures contained prothrombin (0.6 μM), increasing concentrations of short-chain phospholipid, and factor X_a (5 nM) in 50 mM Tris, 0.1 M NaCl, 0.6% PEG (8000), 5 mM Ca^{2+}, pH 7.5 at 37 °C.

Determination of the Stoichiometry of C6PS Binding to Factor X_a. The stoichiometry of short-chain phospholipid binding to factor X_a was determined by equilibrium dialysis experiments in which the difference in total phosphate concentration between the two chambers of the dialysis cell was monitored. Experiments were performed using 2.0 mL Teflon dialysis cells (Spectrum Medical, Los Angeles) with the two cells separated by a 6000−8000 dalton molecular mass cutoff membrane. Both chambers contained 400 μM C6PS[1] in 50 mM Tris, 0.1 M NaCl, 5 mM Ca^{2+}, pH 7.5. Factor X_a was added to half of each of these cells to final concentrations of 30, 50, and 70 μM and allowed to equilibrate with the other half at room temperature for 26 h while being rotated horizontally at 20 rpm. C6PS occupied greater than 80% of protein sites for each protein concentration considered. The difference in total phosphate concentration between the two chambers (ΔP) was then measured by taking eight aliquots (100 μL) out of each chamber and assaying these for total phosphate content according to the method of Chen et al. (*8*). Total phosphate content was also measured for buffer plus protein alone as a control. It is easy to show that ΔP should vary linearly with factor X_a concentration with a slope equal to $n[L]/[k_d(1 + [L]/k_d)]$, where [L] is the free lipid concentration, k_d is the site dissociation constant for lipid binding (taken as 86 μM), and n is the stoichiometry of binding. To estimate n from the slope of a plot of ΔP versus factor X_a concentration, we plotted expected values of ΔP versus factor X_a concentration assuming different values of the stoichiometry ($n = 1$, 2, 3, and 4), with one of these curves matching best the observed data.

Titration Data Analysis. In our titrations of DEGR-X_a, soluble lipids were added to the protein solution, and the observed response was modeled according to a single-site or a two-sequential-site model, as described in detail elsewhere (*25*). For any observable, R (in our case fluorescence intensity or activity), we can describe the response to lipid titration as

$$R = R_0 + \sum_{i=1}^{n} \Delta R_{sat,i} \cdot f_i \qquad (1)$$

where f_i is the fraction of X_a in the ith bound state, R_0 is the response in the unbound state, and $\Delta R_{sat,i}$ is the change in observable due to saturating the ith bound state. For independent sites, the index i refers to individual binding sites, but for linked sites, i refers to a particular arrangement of ligands over available sites.

For a *single-binding-site model*, f is expressed as follows:

$$f = \frac{k_1[L]}{1 + k_1[L]} \qquad (2)$$

and the observable is fit as follows:

$$R = R_0 + \Delta R_{sat} \frac{k_1[L]}{1 + k_1[L]} \qquad (3)$$

where k_1 is the binding constant for occupancy of a single site and [L] is the free concentration of lipid present in the reaction mixture, which under our conditions (0.1 μM factor X_a) is approximately the total added lipid concentration. This is the model used to fit short-chain lipid titrations of the rate of thrombin generation. The same model adequately described DEGR-X_a titrations by some lipids (groups IIB, III, and IV).

For DEGR-X_a titrations by other lipids (groups I and IIA), the *sequential-binding-site model* was required. In this model, occupancy of the first site according to the binding constant k_1 elicits a response $\Delta R_{sat,1}$. Only after the first site is occupied can the second site be occupied according to the binding constant k_{12}, with a response, $\Delta R_{sat,12}$, characteristic of factor X_a with both sites occupied. The observable R can be written as

$$R = R_0 + \frac{\Delta R_{sat,1} k_1[PL] + \Delta R_{sat,12} k_1 k_{12}[PL]^2}{\Theta} \qquad (4)$$

where Θ is a modified grand partition function having one term for every possible bound species:

$$\Theta = 1 + k_1[PL] + k_1 k_{12}[PL]^2 \qquad (5)$$

Note that there is no term for the species with only site 2 occupied. This is the simplest model that we found could account for both the functional and structural responses of factor X_a to soluble phospholipid binding (*25*).

In experiments in which we examined cooperation or competition between two lipids, many more species are possible. In general, for two lipids (e.g., PS and PG), the sequential-binding model leads to six possible species, so that the observed response can be written:

$$R = R_0 + (\Delta R_s k_{1s}[PS] + \Delta R_{ss} k_{1s} k_{12ss}[PS]^2 + \Delta R_{sg} k_{1s} k_{12sg}[PS][PG] + \Delta R_g k_{1g}[PG] + \Delta R_{gg} k_{1g} k_{12gg}[PG]^2 + \Delta R_{gs} k_{1g} k_{12gs}[PG][PS])/\Theta \qquad (6)$$

where

$$\Theta = 1 + k_{1s}[PS] + k_{1s} k_{12ss}[PS]^2 + k_{1g}[PG] + k_{1g} k_{12gg}[PG]^2 + [PS][PG]\{k_{1s} k_{12sg} + k_{1g} k_{12gs}\} \qquad (7)$$

This expression contains 12 parameters: 6 ΔR's and 6 k's. Competition experiments having a simple hyperbolic shape can define two parameters, while S-shaped curves can define three parameters. Thus, in describing two-ligand competition experiments, we fixed parameters associated with binding of a single ligand based on analysis of single ligand experiments. In some cases, we have also made

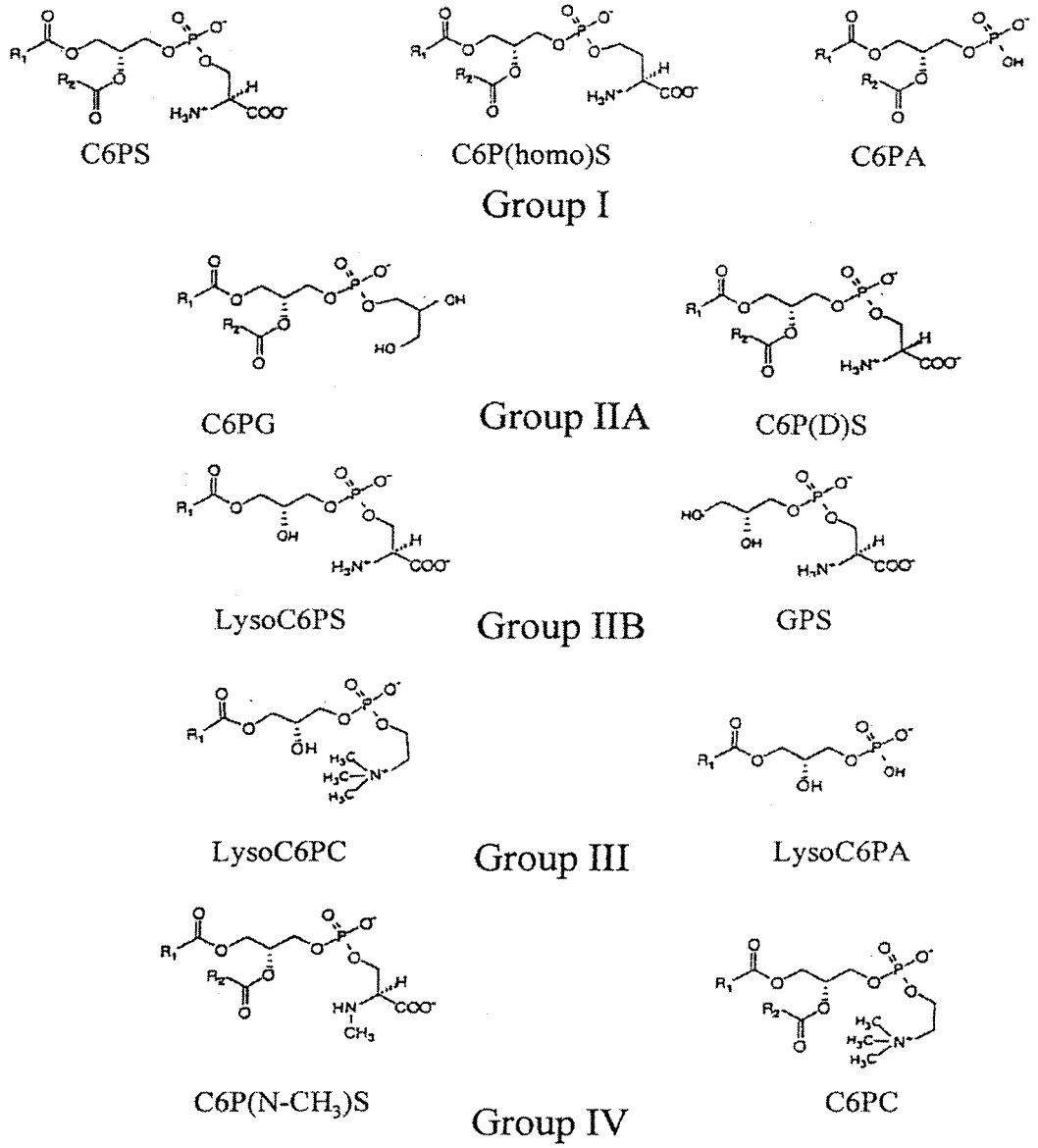

FIGURE 1: Structures of various C6PS analogues used for binding studies are grouped according to their ability to elicit functional and structural responses from factor X_a. R_1=R_2 represents C_5H_{11}.

reasonable assumptions that eliminate some species that are not likely to contribute to the observed response in order to eliminate some parameters. Details of these assumptions are presented under Results.

RESULTS

Synthetic Phospholipids: *The Response of DEGR-X_a Fluorescence to Short-Chain Phospholipids in the Presence of Ca^{2+}*. We have shown previously (*18*, *25*) that the fluorescence of active-site dansylated factor X_a (DEGR-X_a) responds to titration by soluble phospholipids in parallel to other structural (CD spectra) data but in somewhat different fashion than do functional (synthetic substrate hydrolysis, prothrombin proteolysis, autolysis) properties of factor X_a. In this paper, we have used DEGR-X_a fluorescence as a convenient measure of factor X_a structural response to lipid binding and prothrombin activation as the ultimate measure of functional response. We have recorded both the structural and the functional responses of human factor X_a to 11 synthetic, soluble phospholipids. We have grouped the 11 phospholipids according to the responses they elicited upon binding to DEGR-X_a. These groupings are shown in Figure 1. Typical responses of DEGR-X_a to each of these groups in the presence of 5 mM Ca^{2+} are presented in Figure 2A and in the absence of Ca^{2+} in Figure 2B. Results are described for each lipid group.

(A) Group I Lipids. C6PS (closed circles in Figure 2), C6P-(homo)S (not shown), and C6PA (not shown) all produced, at saturating concentration of lipid, nearly a 30% drop in the fluorescence intensity of human DEGR-X_a in the presence of 5 mM Ca^{2+} (Table 1). All Group I lipids also clearly elicited an "S-shaped" response of DEGR-X_a fluorescence that could not be described by a single-site, hyperbolic binding curve. We argue elsewhere, based on the fluorescence of DEGR-X_a, CD spectroscopy, and activity titrations, that this S-shaped binding isotherm is due to sequential occupancy of at least two linked lipid binding sites on factor X_a, each eliciting a different structural response (*25*). Occupancy of the first of these sites elicits a structural response that leads to dimer formation that produces a

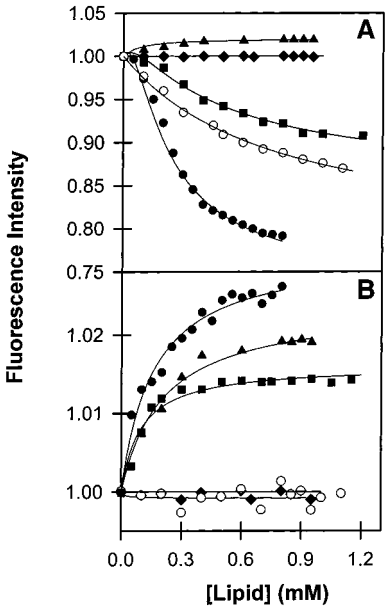

FIGURE 2: DEGR-X_a (100 nM) in 50 mM Tris, 0.1 M NaCl, pH 7.5, was titrated with C6PS (filled circles), C6lysoPA (diamonds), C6PC (triangles), GPS (open circles), and C6P(D)S (closed squares) in the presence (frame A) and absence (frame B) of 5 mM Ca^{2+} at 37 °C. Fluorescence intensities of DEGR-X_a were measured after an equilibration period of 4 min after each microliter addition of the lipids as described in detail under Methods. All lipids used for this study were divided into four groups (I, II, III, IV, see Figure 1), depending upon the fluorescence response of DEGR-X_a titrated with these lipids (Table 1). Lines drawn through the data were obtained by nonlinear regression of the models described under Methods to the data shown. Parameters from these fits are summarized in Table 1. Note that data for C6PS are presented only to 0.8 mM lipid, since all three Group I lipids had CMCs in the range 0.8−0.9 mM under our experimental conditions, as judged both by ANS fluorescence and by a discontinuity in the DEGR-X_a fluorescence response. The CMC of C6PS in the presence of factor X_a and 5 mM Ca^{2+} has also been characterized by proteolytic activity measurements as 0.8 mM (*18*). Data above the CMC cannot be interpreted in terms of binding of individual C6PS molecules.

positive change in DEGR-X_a fluorescence. Occupancy of the second site leads to a structural change that produces a negative change in DEGR-X_a fluorescence (*25*). All three data sets were fit adequately (solid curve through filled circles in Figure 2A) by a sequential binding model (*25*). The parameters resulting in best fits to the data are summarized in Table 1.

(B) Group II Lipids. The responses of DEGR-X_a fluorescence to C6P(D)S (squares) and GPS (open circles) in the presence of Ca^{2+} are also recorded in Figure 2A. Binding isotherms with C6lysoPS and C6PG (not shown) were completely analogous to those with GPS and C6P(D)S, respectively. Titration of DEGR-X_a with Group II lipids in the presence of Ca^{2+} produced in all cases only a bit more than half the fluorescence decrease seen for Group I lipids (Figure 2A and Table 1). With regard to the shape of the binding isotherm, Group II lipids showed two behaviors. *Group IIA* lipids {C6PG (not shown) and C6P(D)S (squares)}, like Group I lipids, elicited an S-shaped response in the fluorescence intensity of DEGR-X_a that required the sequential-site model for description. *Group IIB* lipids {GPS (open circles) and C6lysoPS (not shown)} caused about the same decrease (∼15−22%) in the emission intensity of DEGR-X_a as did Group IIA lipids but with a simple, single-site, hyperbolic response curve in the presence of Ca^{2+}. Binding parameters derived from fitting these curves to these models are summarized in Table 1, and the best-fit curves are given in Figure 2 for C6P(D)S and GPS.

(C) Group III and Group IV Lipids. Figure 2A,B also shows the emission intensity of DEGR-X_a when titrated with representatives of these two groups of lipids. Group III lipids {C6lysoPC (not shown) and C6lysoPA (diamonds)} showed no change at all in the emission intensity of DEGR-X_a in the presence of Ca^{2+} (Figure 2A). This indicates either that the group III lipids have no interaction with factor X_a or that any interaction that does occur causes no change in the active-site conformation of factor X_a. Group IV lipids {C6PC (closed triangles) and C6P(N-Me)S (not shown)}, unlike the other three lipid groups, produced a small *positive* and simple hyperbolic response in DEGR-X_a fluorescence (Figure 2A). The parameters characterizing these binding isotherms are summarized in Table 1.

Stoichiometry of C6PS Binding. In describing the S-shaped fluorescence response curves for Group I and Group IIA lipids, we have used a model that assumes sequential occupancy of two linked sites (*25*). The existence of two C6PS sites on bovine factor X_a has been confirmed by equilibrium dialysis (*24*), and we confirm this in Figure 3 for human factor X_a by the same method (see Methods).

The Response of DEGR-X_a Fluorescence to Short-Chain Phospholipids in the Absence of Ca^{2+}. We showed previously that the two lipid binding sites on factor X_a had different Ca^{2+} dependencies (*25*). A Ca^{2+}-dependent site exists in the EGF domain pair and has different responses in the presence and absence of Ca^{2+}, while the Ca^{2+}-requiring site is in the catalytic domain and is silent in the absence of Ca^{2+} (*24*, *25*). In the absence of Ca^{2+}, our data (Figure 2B and Table 1) show that the emission intensity of DEGR-X_a increased slightly (∼1.5−3%) upon addition of Group I, Group IIA, or Group IV lipids to human DEGR-X_a, and this event could be described by a single-site, binding model with $k_d \approx 100-300$ μM (Table 1). However, DEGR-X_a fluorescence remained essentially unchanged in the presence of Group IIB lipids such as C6lysoPS (not shown) or GPS (open circles) (Table 1). Since Group I [C6PS and C6P(homo)S] and Group IIA lipids [C6PG and C6P(D)S] both elicited an S-shaped response in DEGR-X_a fluorescence in the presence of Ca^{2+}, this suggests that they bind to both the Ca^{2+}-dependent and the Ca^{2+}-requiring sites in the presence of Ca^{2+} but bind only to the Ca^{2+}-dependent site in the absence of Ca^{2+} (site 2 in Table 1). Group IV lipids [C6PC or C6P(N-Me)S] elicited nearly the same small positive fluorescence response from DEGR-X_a in the absence of Ca^{2+} (Figure 2B) as seen in its presence (Figure 2A), implying that these lipids bind only to the Ca^{2+}-dependent site. Group III lipids (C6lysoPC and C6lysoPA) showed no change in the emission intensity of DEGR-X_a in the absence of Ca^{2+} (Figure 2B), just as they elicited no response in the presence of Ca^{2+}. We conclude that all lipids having a diacylglycerol (DAG[1]) backbone structure (i.e., two acyl chains, independent of the headgroup species or charge) bound to the Ca^{2+}-dependent site in the EGF domain pair in both the presence and absence of Ca^{2+}. Lipids having a glycerolphosphorylserine (GPS) headgroup structure seem to bind to the Ca^{2+}-requiring site in the catalytic domain, but bind to the Ca^{2+}-dependent site only when they have two acyl chains, i.e., a DAG backbone.

Table 1: Parameters Associated with the Various PS Analogues Binding to Factor X_a and with the Rate of Prothrombin Activation

		site dissociation constants[a] in presence of Ca^{2+}		DEGR-X_a fluorescence intensity change: ΔF_{sat}[a]		site dissocn constants[a] in absence of Ca^{2+}, k_{d1}[a] (μM)	DEGR-X_a fluorescence intensity change in absence of Ca^{2+}, ΔF_{sat}[a] (fraction of F_0)	titration of prothrombin activation rate,[b] app k_d[a] (nM/min)//(μM)
	lipids	k_{d1} (μM)	k_{d12} (μM)	site 1 (fraction of F_0)	site 2 (fraction of F_0)			
Group I	C6PS	86[c]	203 ± 21	0.050 ± 0.002	−0. 29 ± 0.01	155 ± 19	0.031 ± 0.001	1.0 ± 0.1// 86 ± 5
	C6P(homo)S	97[c]	136 ± 11	0.084 ± 0.002	−0.27 ± 0.01	102 ± 19	0.016 ± 0.001	1.0 ± 0.2// 97 ± 6
	C6PA	98[c]	176 ± 11	0.045 ± 0.002	−0.30 ± 0.01	293 ± 19	0.019 ± 0.001	1.0 ± 0.1// 98 ± 6
Group IIA	C6PG	160[c]	330 ± 19	0.040 ± 0.009	−0.17 ± 0.006	90 ± 18	0.016 ± 0.006	NC[e]// 160 ± 20[d]
	C6P(D)S	71[c]	470 ± 75	0.030 ± 0.012	−0.15 ± 0.013	97 ± 15	0.016 ± 0.0006	0.20 ± 0.1// 71 ± 9[d]
Group IIB	C6lysoPS	NA[f]	680 ± 75	NA	−0.17 ± 0.009	NA	NC	0.10 ± 0.09// ND[g]
	GPS	NA	770 ± 70	NA	−0.22 ± 0.01	NA	NC	0.11 ± 0.02// ND
Group III	C6lysoPC	NA	NA	NC	NC	NA	NC	NC//ND
	C6lysoPA	NA	NA	NC	NC	NA	NC	NC//ND
Group IV	C6PC	203 ± 27	NA	0.024 ± 0.001	NC	203 ± 27	0.024 ± 0.001	NC//340[d]
	C6P(N-Me)S		185 NA ± 27		0.007 NC ± 0.001	185 ± 27	0.007 ± 0.001	NC//ND

[a] Site dissociation constants, k_{d1}, k_{d2}, and k_{d12}, and ΔF_{sat} values were obtained by fitting the experimental data to the binding models discussed under Methods and in the text. In all cases, parameters that were determined by regression analysis all passed *t*-tests with $P < 0.001$, where P is the probability that the term defined by a coefficient does not contribute to the variation of y with x. Standard errors of the parameter values were obtained from the regression analysis. [b] Prothrombin activation by factor X_a was measured as described under Methods. Values reported are those observed at saturating short-chain lipid concentration for C6PS, C6PA, and C6P(homo)S. All others were measured at 1 mM added soluble lipid. [c] k_{d1} values were fixed during the analysis with the binding constant obtained from titration of activity. The errors on these parameters were obtained from fitting procedures and are given in the far right-hand column. [d] k_1 was determined from a titration of amidolytic activity against the synthetic substrate S-2765. Many lipids that do not enhance the proteolytic activity do alter the amidolytic activity, and the apparent k_d's from the two types of activity responses to C6PS are similar (*18*). [e] NC: no change is observable. [f] NA: not applicable. [g] ND: not determined.

Effects of Short-Chain Phospholipids on Factor X_a Proteolytic Activity. We also screened the different C6PS analogues for their abilities to alter the proteolytic activity of factor X_a toward prothrombin. For each lipid species, the rate at which prothrombin was activated to meizothrombin plus thrombin was measured (see Methods) at increasing lipid concentrations. The resulting initial rates for Group I lipids showed saturating behavior when plotted as a function of short-chain lipid concentration with a discontinuity at the CMC of the particular short-chain lipid, as previously described in detail for C6PS (*18*). At concentrations below the CMC, all of these were well described by a single-site-binding model, with the saturating rates and apparent k_d values summarized in Table 1. These results show that all the lipids in Group I were equally able to enhance prothrombin activation, and with very similar apparent site dissociation constants. This rate (5×10^3 M^{-1} s^{-1}) is much smaller than is seen for the full prothrombinase assembled in solution under the influence of C6PS (10^8 M^{-1} s^{-1}) (*19*) but is still 60-fold greater than seen in the absence of lipid (*18*) and within a factor of 2−3 of that seen with PS-containing membranes without factor V_a (*1*). Clearly, binding of C6PS or other Group I lipids accounts for most of the contribution of membranes to factor X_a activation, and binding of C6PS-activated factor V_a accounts for the rest (*19*).

Although both C6PG and C6P(D)S (Group IIA) caused similar S-shaped decreases in the fluorescence intensity of DEGR-X_a, only C6P(D)S caused an increase in factor X_a activity (Table 1), about 20% of that recorded in the presence of Group I lipids. We conclude that C6PG and C6P(D)S, despite the similarity in their effects on DEGR-X_a fluorescence, cause different conformational changes in factor X_a, since they did not elicit the same changes in activity.

The Group IIB lipids (C6lysoPS and GPS) elicited at 1 mM concentration only about 10% of the proteolytic response of Group I lipids and apparently incomplete changes in the active site of factor X_a. The Group III lipids (C6lysoPC and C6lysoPA) elicited no structural or functional response in factor X_a, and, indeed, there is no evidence that these lipids bind at all to the protein. Both Group IV lipids [C6PC and C6P(N-Me)S] also seemed to induce a common structural change but no change in factor X_a proteolytic activity.

Cooperative Effects of Phospholipids on DEGR-X_a. To summarize our results to this point (Table 1), it seems that the Ca^{2+}-requiring site recognizes most negatively charged lipids and, at minimum, the negatively charged GPS, while the Ca^{2+}-dependent site recognizes at a minimum the DAG moiety. The two-site, sequential binding model that we have previously proposed (*25*) states that the ability of C6PS to occupy the GPS site should depend on whether the first site is occupied with a DAG-containing lipid. To test this proposal, we titrated DEGR-X_a with sufficient C6PC (0.2 mM) to saturate ~50% of the first type of site on factor X_a (based on a single-site dissociation constant of ~200 μM; Table 1) and then titrated with C6PS. The resulting decrease in DEGR-X_a fluorescence is presented in Figure 4A. The response to C6PS approximated a simple hyperbolic behavior (dotted line in Figure 4A; apparent $k_d = 270$ μM, $\Delta F_{sat} = -0.26$) instead of the S-shaped behavior seen in Figure 2A. This result implies that a mixed lipid species must be formed in this experiment, with the DAG site occupied initially by C6PC and linked to the GPS site that could be occupied by

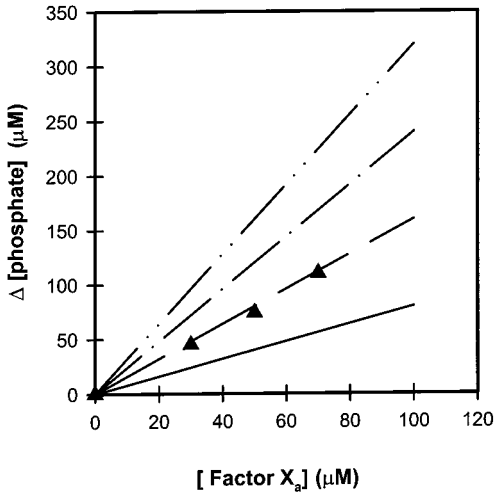

FIGURE 3: Predicted values of the difference of phosphate concentrations (Δ[phosphate]) between the two chambers of equilibrium dialysis cells (as described under Methods) are plotted as a function of increasing concentrations of factor X_a for four assumed values of stoichiometry [$n = 1$ (solid line), 2 (dashed line), 3 (dash−dot line), and 4 (dash−dot−dot line)]. Experiments were performed at 400 μM C6PS, a concentration sufficient to occupy greater than 80% of the binding sites on the factor X_a present at any of these three protein concentrations. Closed triangles show the experimentally determined Δ[phosphate] values, showing clearly that the stoichiometry of C6PS binding to factor X_a is 2.

C6PS directly since the DAG site was already occupied. To test the feasibility of this explanation, we fit the data to the multiple-ligand model described under Methods (eq 6). In doing so, we allowed for four species: X_a·PC, X_a·PS, X_a·PC·PS, and X_a·PS·PS, and fixed within experimentally observed ranges all the known parameters from Table 1 (k_{1s}, k_{1c}, k_{12ss}, ΔR_s, ΔR_c, ΔR_{ss}, R_0). The species X_a·PC·PC and X_a·PS·PC were excluded based on our results that the second site does not bind C6PC. Thus, we adjusted only two mixed-species parameters (k_{12cs} and ΔR_{cs}) to obtain the best fit (solid line through the data; parameters given in Table 2). Note that k_{d12cs} obtained from this fit is about the same as k_{d12ss} given in Table 1 when C6PS occupies site 1, consistent with the hypothesis that C6PC meets the minimal requirement for site 1. In this description, the lack of an S-shaped titration curve resulted from replacement of the species X_a·PS (positive ΔF) with the X_a·PC·PS species (negative ΔF). We also attempted to fit our results without the X_a·PC·PS species but with the parameter constraints described above. The results (dashed line in Figure 4A) confirm the necessity of including the mixed species to explain the results of this experiment if one assumes parameters that are consistent with our single-lipid titrations.

To test whether the putative GPS-requiring site might elicit a full structural response when C6PC was present to occupy the DAG site, an experiment similar to that recorded in Figure 4A was performed, but with GPS as the second titrant. GPS contains the glycerol backbone plus headgroup of C6PS without its acyl chains. The results are shown as open circles in Figure 4B and clearly follow a simple hyperbolic behavior (apparent $k_d = 260$ μM, $\Delta F_{sat} = -0.29$). The curve plotted in Figure 4B was predicted by the mixed-lipid model described for Figure 4A. This required adjusting only two parameters (k_{12cg} and ΔR_{cg}) that are given in Table 2. These parameter values indicate that the k_{d12cg} (140 μM) for GPS

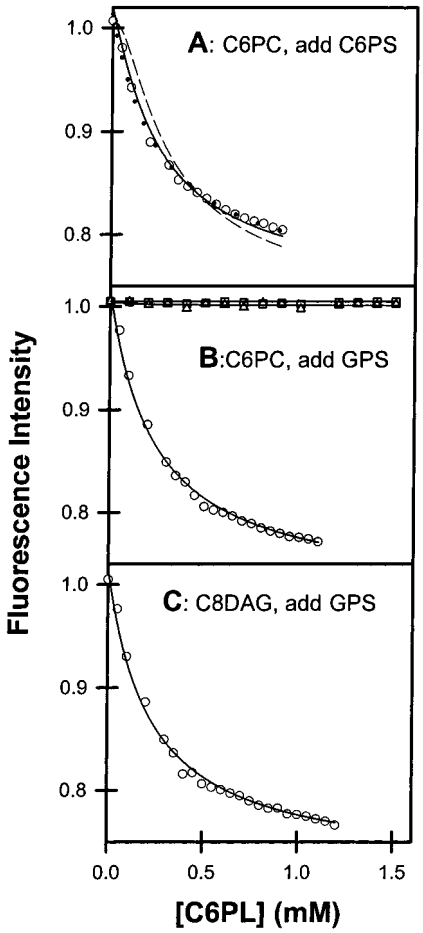

FIGURE 4: Effect of DAG-containing lipids on the response of DEGR-X_a fluorescence to C6PS and DAG. DEGR-X_a (100 nM) in 50 mM Tris, 0.1 M NaCl, pH 7.5, was preincubated for 30 min with 0.2 mM C6PC (frames A and B) or 0.2 mM C8diacylglycerol (frame C) in the presence of 5 mM Ca^{2+} at 37 °C. At the end of that initial incubation period, changes in fluorescence intensities were measured with increasing concentrations of (frame A) C6PS, or (frame B) GPS (circles), *O*-phospho-L-serine (squares), or L-serine (triangles). Frame C shows the change in DEGR-X_a fluorescence as a function of increasing concentrations of GPS in the presence of 0.2 mM C8DAG. The solid curves drawn through the circles indicate the fit of the data to a multi-species binding model (eq 6 under Methods), with parameters fixed as described in the text. The adjusted k_d values and fluorescence changes at saturation obtained from these fits are summarized in Table 2. The dashed line in frame A shows the result of an attempt to explain the data without including the mixed species (X_a·PC·PS). The dotted curve in frame A shows the result of fitting a simple hyperbola to the data.

binding to site 2 with site 1 occupied by C6PC was much smaller than the k_{d2g} obtained for GPS binding to site 2 in the absence of C6PC (770 μM; Table 1). Indeed, it was comparable to the k_{d12ss} for occupancy of site 2 by C6PS when site 1 was occupied by C6PS (203 μM; Table 1). Since GPS does not bind to site 1, it is clear that occupancy of site 1 by C6PC altered the interaction of site 2 with GPS, demonstrating the linkage between these sites. Also shown in Figure 4B are results obtained with *O*-phospho-L-serine (squares) and L-serine (triangles), structures even smaller than GPS. These compounds did not cause any change in the DEGR-X_a fluorescence intensity even when the first site was occupied by C6PC (Figure 4B). Taken together, these results confirm that GPS is the minimum negatively charged

Table 2: Analysis of Cooperative and Competitive Binding of Pairs of Lipids to DEGR-X_a

experiment	lipids	site dissociation constant, k_{d12}[a] (μM)	DEGR-X_a fluorescence intensity change: ΔF_{sat12}[a] (fraction of F_0)	initial rate of prothrombin activation[b] (nM/min)
cooperative binding	C6PC; add C6PS	133 ± 29	−0.26 ± 0.01	0.82 ± 0.1
	C6PC; add GPS	140 ± 10	−0.29 ± 0.01	0.09 ± 0.08
	DAG; add GPS	131 ± 10	−0.28 ± 0.01	0.08 ± 0.1
competitive binding	C6PS; add C6PG			ND[d]
	species:			
	X_a·PS·PG	800 ± 360[c]	−0.28 ± 0.03	
	X_a·PG·PS	>1200	ND	
	C6PS; add C6lysoPS	92 ± 9	−0.26 ± 0.01	ND
	C6PS; add GPS	47 ± 6	−0.29 ± 0.01	ND

[a] Site dissociation constants and ΔF_{sat12} values were obtained by fitting the experimental data to the multiple-ligand model (eq 6) discussed under Methods. In all cases, as many parameters as possible were fixed based on independent experiments (see Results), so that most parameters that were determined by regression analysis l passed *t*-tests with $P < 0.001$. Standard errors of the parameter values were obtained from the regression analysis. [b] Prothrombin activation by factor X_a was measured as described under Methods. Values reported were measured at 1 mM added soluble lipid. [c] Binding constant for PG binding to X_a·PS (k_{12sg}) was fixed based on analysis of the data in Figure 5. The *P* value for k_{12sg} was <0.05. [d] ND: not determined.

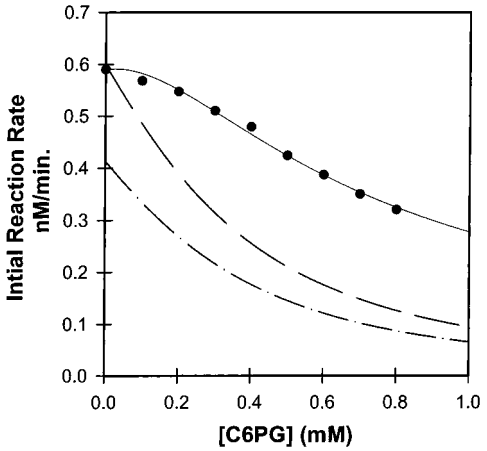

FIGURE 5: Inhibition of C6PS-induced rate enhancement of prothrombin activation by phosphatidylglycerol. The initial rate of thrombin plus meizothrombin active site appearance (prothrombin activation) was determined using the synthetic thrombin substrate S-2238 as described under Methods. Concentrations of prothrombin (0.6 μM), factor X_a (5 nM), and C6PS (0.2 mM) in 50 mM Tris, 0.1 M NaCl, 0.6% PEG, and 5 mM Ca^{2+}, pH 7.4 at 37 °C, were fixed while the rate of activation was monitored as a function of increasing concentrations of C6PG. Attempts were made to fit the data with models that assumed increasing numbers of mixed-lipid factor X_a species present. The dashed−dotted line was obtained by assuming that only X_a·PS·PS was present and contributed to the observed activity. The dashed line was obtained by assuming that both X_a·PS·PS and X_a·PS contributed to activity. The solid line was obtained by assuming that X_a·PS·PS, X_a·PS, and X_a·PS·PG all contributed to the observed activity. The activities of these species that led to the calculated solid line were 1.0, 0.44, and 1.0 nM/min, respectively. The binding constant k_{12sg} adjusted to 800 μM.

structure that can be recognized by the second, Ca^{2+}-requiring site on factor X_a and the structural response to occupancy of this site by either GPS or C6PS depends on occupancy of the DAG site.

We have also tested whether the DAG moiety is the minimum structure required for the tighter, and Ca^{2+}-dependent, site. Figure 4C shows the effect of GPS on the fluorescence intensity of DEGR-X_a when the Ca^{2+}-dependent regulatory site is occupied by C8DAG. The low solubility of this lipid made it impossible to fully characterize its binding to factor X_a, but from what we could learn, its behavior paralleled that of C6PC. Thus, the concentration of C8DAG used (0.2 mM) was chosen as likely to half-saturate the first lipid site based on assuming that C8DAG had about the same k_d as for C6PC. This concentration is well below the CMC (350−400 μM) of this fairly insoluble lipid. The response of factor X_a to GPS titration in the presence of 0.2 mM C8DAG was very similar to the response seen on adding GPS in the presence of C6PC (compare Figure 4B and Figure 4C). The fitted curve in Figure 4C and the parameters in Table 2 were obtained as described for Figure 4A,B. These results clearly indicate that the phosphorylcholine headgroup is not needed and that only the DAG moiety is needed to activate the GPS site on factor X_a.

Although the DAG moiety is the minimal structure needed to occupy site 1, can it elicit a functional response? The proteolytic activity seen for factor X_a in the presence of 0.2 mM C6PC and 1 mM C6PS (0.82 nM/min; Table 2) was somewhat less than that seen for factor X_a activated by C6PS alone (1 nM/min; Table 1). This is because about 80% of factor X_a is predicted to be present as the X_a·PS·PS species under these conditions, with the remainder of factor X_a present as X_a·PS or X_a·PC·PS. This implies that the X_a·PC·PS species has little or no activity. Furthermore, although occupancy of site 2 by GPS elicits a full DEGR-X_a fluorescence response in the presence of C6PC (Table 2; Figure 4B), the proteolytic response obtained with this combination of lipids was only 10% of that seen for C6PS, consistent with the response seen for GPS alone (Table 1). Similarly, the DAG/GPS lipid pair also elicited only 10% of the full increase in factor X_a proteolytic activity seen for C6PS alone (Table 2). Since only about 15% of factor X_a is present as X_a·GPS under the conditions of the activity assay, it must be that the remainder of the factor X_a (present as X_a·PC·GPS or X_a·DAG·GPS) has about the same activity as X_a·GPS. Again, this suggests that, although DAG or C6PC in site 1 is sufficient to elicit a structural response and to trigger occupancy of the GPS site, a structural change that produces a full functional response probably requires that site 1 be occupied by an appropriate acidic lipid [C6PS, C6PA, or C6P(homo)S], not just by its minimal ligand, DAG. These results suggest that occupancy of site 1 by C6PS is of primary consideration in determining factor X_a activity.

Specific Requirement for C6PS at Site 1. To test whether one or both sites must be occupied by C6PS in order to elicit a full proteolytic or structural response, we performed two sets of experiments with C6PG, a Group IIA lipid (Table 1) that binds to both site 1 and site 2, but produces a fluorescence decrease only about 60% of that produced by C6PS and no activity enhancement. Figure 5 shows the results of a competition experiment in which we titrated 5

nM factor X_a with C6PG in the presence of 200 μM C6PS (sufficient C6PS to produce 78% of the total possible enzyme up-regulation). In searching for a quantitative description of these data, we fixed from Table 1 all the parameters that could be fixed based on other experiments (k_{1s}, k_{1g}, k_{12ss}, k_{12gg}, ΔA_{ss}), and allowed for the existence of all six possible bound species indicated in eq 6 (Methods) but assumed that only some of them were active. Initially, we tried to fit these data assuming that only the species X_a·PS·PS was fully active, with its activity ($\Delta A_{ss} = 1$ nM/min) defined by the experiments summarized in Table 1. The fit shown as the dash−dot line in Figure 5 was obtained with k_{12gs} close to 0. The values assigned to k_{12gs} and k_{12sg} had little effect on the quality of the fit. Any description of the data obtained with only X_a·PS·PS as an active species was clearly inadequate.

We considered next that both X_a·PS·PS and X_a·PS might contribute to factor X_a activity, with the activity of X_a·PS treated as an adjustable parameter. With $\Delta A_s = 0.44$ nM/min, we matched the initial point at [PS] = 200 μM and [PG] = 0, but could not explain the full response curve (see dashed curve in Figure 5). Only when X_a·PS·PS, X_a·PS, and X_a·PS·PG were all considered as being active species (ΔA_s and ΔA_{ss} fixed at 1 and 0.44 nM/min) were our observations well described (solid line in Figure 5). The activity response curve was best described with the activity of the X_a·PS·PG species equal to that of the X_a·PS·PS species (1.0 nM/min) and the value of k_{d12sg} taken as 475 μM. The fact that the activity of X_a·PS·PG was approximately that of X_a·PS·PS and that the activity of the X_a·PS·species was only 0.44 nM/min means that the presence of C6PG in site 2 was both necessary and sufficient to induce full activity as long as C6PS was in site 1. The fact that C6PG in both sites led to no increase in activity indicates that the functional response of factor X_a depends on C6PS occupying site 1, as indicated by the results in Figure 4. When a second mixed lipid species (Xa·PG·PS) was considered to be active, no improvement in fit was obtained, and the activity of this species adjusted to roughly 0 nM/min, also consistent with the need to fill site 1 with PS to obtain maximal proteolytic activity.

The results described above predict that combinations of C6PS binding to site 1 and Group II or III lipids binding to site 2 should be able to cause changes in the structure of factor X_a's active site comparable to that recorded for DEGR-X_a·PS·PS. The experiments presented in Figure 6 test this prediction. Upon addition of C6PG (Figure 6A) to DEGR-X_a that was partially saturated with 200 μM C6PS, the fluorescence intensity of DEGR-X_a decreased in a biphasic fashion toward a saturating value. Because micelle formation would not allow us to reach saturation, we had to extract the structural response of the mixed-lipid species from a quantitative description of our results (eq 6). First, we assumed (as in Figure 5A) that no mixed-lipid species could form. This produced a clearly unacceptable description (dashed line in Figure 6A). Next, we allowed for all six possible bound species. For these calculations, we fixed all parameters that could be determined based on other experiments [k_{1s}, k_{1g}, k_{12ss}, ΔR_s, ΔR_g, ΔR_{ss}, ΔR_{gg} (Table 1), and k_{d12sg} (Table 2)], and varied k_{12gs}, ΔR_{sg}, and ΔR_{gs}. The data were not sufficient to define all three parameters, but in various attempts to fit the data, the species X_a·PG·PS consistently contributed insignificantly to the response. When

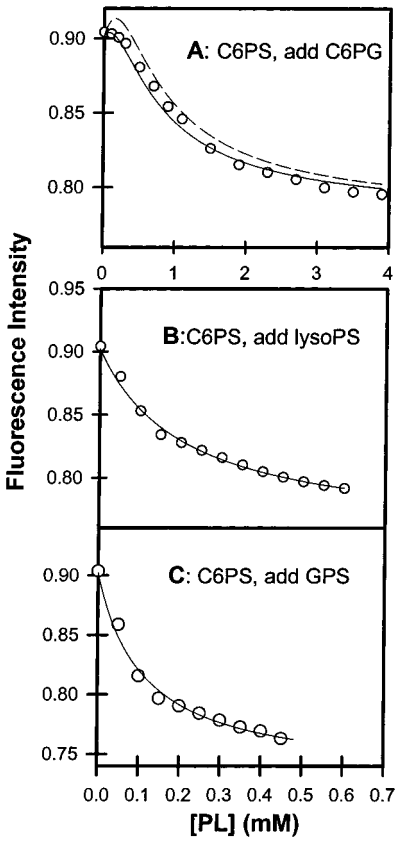

FIGURE 6: Effect of C6PS on the response of DEGR-X_a fluorescence to C6PG, lysoPS, and GPS. DEGR-X_a (100 nM) in 50 mM Tris, 0.1 M NaCl, pH 7.5, was preincubated for 30 min with 0.2 mM C6PS in the presence of 5 mM Ca^{2+} at 37 °C. At the end of that initial incubation period, changes in fluorescence intensities were measured at 37 °C with increasing concentrations of C6PG (frame A) and C6lysoPS (frame B). The solid lines passing through the curves represent fits obtained using the multiple ligand binding equation (eq 6), accounting for all species allowed by our model for lipid specificity of the factor X_a sites. The dashed line in frame A was obtained by assuming that no mixed species were present in the reaction mixture and only X_a·PS·PS, X_a·PS, X_a·PG·PG, and X_a·PG contributed to the observed fluorescence response. Parameters fixed for these fits are given in the text. The mixed species dissociation constants and response parameters (ΔF_{sat12}) that could not be fixed based on other experiments were adjusted to obtain a best fit, with those resulting in the solid lines being reported in Table 2.

this species was eliminated, regression of the model to the data defined a change in DEGR-X_a fluorescence for the mixed-lipid species ($\Delta R_{sg} = -0.28$ in Table 2) within the range of values for saturating both sites with Group I lipids (−0.27 to −0.3; Table 1). This is significantly different from the values obtained for Group IIA lipids (−0.015 to −0.22; Table 1). Group IIB lipids (lysoPS and GPS) gave simpler response curves (Figure 6B,C), presumably because they bind more tightly to site 2 when C6PS occupies site 1 (Table 2). However, the responses of DEGR-X_a fluorescence to occupancy of site 2 were, as for C6PG, like those to Group I rather than Group II lipids (Table 2). We conclude that, as for proteolytic activity, occupancy of site 1 by C_6PS is the key event leading to a full change in structure of factor X_a's active site. The nature of the response depends on the lipid in site 2, with the maximal response seen only when the GPS requirement of site 2 is met.

DISCUSSION

We have shown that C6PS induces structural changes in factor X_a, probably by occupying two linked binding sites in a sequential fashion with different responses from both sites (*25*). One site is located in the EGF domain pair and responds differently in the presence and absence of Ca^{2+}, while a second site requires Ca^{2+} and is located in the catalytic domain (*24*). Of course, prothrombin also binds to PS-containing membranes, but we have demonstrated previously that the C6PS effects reported here and elsewhere are due to sites on factor X_a and not on prothrombin (*18, 24, 25*). We come to the following conclusions about the ligand requirements and linkage of these factor X_a regulatory sites:

(1) The two lipid binding sites on factor X_a have different ligand specificities, one requiring at least a diacylglycerol (DAG) moiety and the other acidic phospholipids, minimally a GPS moiety. One site is occupied in the presence of or absence of Ca^{2+} but with different structural responses and affinities. This follows from previous observations (*25*) and from the analysis summarized in Table 1. A detailed quantitative description is not necessary to reach this conclusion. One need only acknowledge that the S-shaped binding isotherms that we have seen for Group I and Group IIA lipids in the presence of Ca^{2+} must involve binding to both sites, while the simple hyperbolic responses seen in the absence of Ca^{2+} imply only one site. Since all these lipids possess the common structural feature of a diacylglycerol backbone, we have termed this Ca^{2+}-dependent (but not requiring) site the DAG site. This site resides in the EGF domain pair but achieves its full affinity only when this pair is linked covalently to the Gla domain (*24*).

Occupancy of the second site requires Ca^{2+}. This conclusion also derives from previous studies (*24, 25*) and from the data in Figure 2 and Table 1. Since GPS elicits a simple hyperbolic response from DEGR-X_a in the presence of Ca^{2+} but no response without Ca^{2+}, we have termed the Ca^{2+}-requiring site the GPS site. However, this site is not absolutely specific for the GPS moiety. Acidic lipids not having this moiety {C6PA, C6PG, C6P(homo)S} can occupy this site. But this site does not bind just any acidic lipid, since C6P(N-Me)S does not occupy the site. Apparently, the specificity is mainly for glycerophosphate, although this group can be esterified to a number of alcohols (glycerol, serine, homoserine) as long as they are not too bulky. This site seems not to be primarily responsible for control of factor X_a activity (*24, 25*).

(2) Occupancy of the GPS site is altered by binding of ligands to the DAG site. As a result of earlier studies, these sites were viewed as being occupied in a roughly sequential fashion, with the DAG site (the tighter of the two) being occupied first and the GPS site normally being occupied after the first is occupied (*25*). This sequential-occupancy model was not absolutely demonstrated by our earlier studies and is only a convenience for describing the observed behavior of the system (*25*). Here, we have reported experiments that make it clear that the GPS site can be occupied at very low affinity without occupying the DAG site (Table 1; Group IIB lipids). However, the GPS site is occupied at much higher affinity when a lipid is present to occupy the DAG site (Tables 1 and 2). This demonstrates the linkage between these two sites and provides strong support for the sequential-site model as a reasonable approximation to describing the binding of C6PS by factor X_a (*25*).

(3) The DAG site appears to be responsible for factor X_a activation, but full activation is achieved only when this site is occupied with PS, and another acidic lipid is in the second site. As mentioned above, occupancy of the GPS site, even without occupancy of the DAG site by Group IIB lipids, clearly produces some (ca. 10% of maximal) enhancement of proteolytic activity. Thus, the activity enhancement is not due, as previously thought (*25*), only to occupancy of the DAG site. However, occupancy of site 2 by membrane-associated PS should not produce physiologically significant factor X_a activity enhancement. This site is located in the catalytic domain (*24*), which is far from a membrane surface (*14*) and thus should not be involved in PS regulation of factor X_a activity. What then might be the physiological role of the GPS site? This site, in human factor X_a, involves a residue (Tyr 99 in the chymotrypsin numbering system) (*24*) that is very near residues that have been implicated in factor V_a binding (*7*). We know that occupancy of the DAG site stimulates increased affinity of the GPS site and leads to factor X_a dimers (*25*). We also know that C6PS binding to factor X_a stimulates higher affinity association with factor V_a (*19*). Thus, it may be that the GPS site is actually part of a protein−protein interaction region involved in factor V_a binding and in factor X_a dimerization when factor V_a is not present. Just as factor V_a binding to factor X_a's catalytic domain leads to enhanced proteolytic activity (*6*), C6PS binding to a similar region of factor X_a might lead to some enhancement of activity. Whatever the reason for the effects of C6PS binding to the GPS site, generation of full proteolytic activity required that both sites were occupied, but, most importantly, that C6PS or one of the other Group I lipids occupied the DAG site (Figure 5, Table 2). This makes the overall requirement for up-regulating factor X_a quite specific for PS, as we have previously observed (*18*), and means that the DAG site is critical in regulating activity.

Despite the clear requirement for occupancy of both sites for full proteolytic activity, we have reported that titrations of both bovine and human factor X_a activity fit very well a single-site-binding model (*18, 25*). It seems this occurs for three reasons. First, occupancy of site 1 is the critical step in regulating activity, since it must be occupied for site 2 to be occupied with reasonable affinity [(*25*); Table 2]. Second, k_{d12} is not too much larger than k_{d1} (as demonstrated in Table 1). Finally, the response of both of the sites is the same (i.e., both enhance activity), as recorded in Table 1. These latter two observations make it difficult to distinguish between a single-site and two-site binding model. To demonstrate this, we modeled the activity of factor X_a in response to addition of C6PS based on the parameters values ($k_{d1} = 86\ \mu M$; $k_{d12} = 203\ \mu M$; $\Delta A_1 = 0.44$ nM/min, and $\Delta A_1 = 1.0$ nM/min) we obtained here (Tables 1 and 2). The resulting increase in activity followed nearly perfectly a single site behavior, with an apparent k_d of 83 μM, nearly exactly as we have reported (*25*).

ACKNOWLEDGMENT

Mass spectral data were obtained at the Michigan State University Mass Spectrometry Facility which is supported, in part, by a grant (DRR-00480) from the Biotechnology

Research Technology Program, National Center for Research Resources, National Institutes of Health.

REFERENCES

1. Banerjee, M., Majumder, R., Weinreb, G., Wang, J. F., Majumder, R., and Lentz, B. R. (2002) *Biochemistry 41*, 950−957.
2. Bartlett, G. R. (1959) *J. Biol. Chem. 234*, 466−468.
3. Basse, F., Gaffet, P., Rendu, F., and Bienvenue, A. (1993) *Biochemistry 32*, 2337−2344.
4. Bevers, E. M., Comfurius, P., and Zwaal, R. F. (1983) *Biochim. Biophys. Acta 736*, 57−66.
5. Bode, A. P., Sandberg, H., Dombrose, F. A., and Lentz, B. R. (1985) *Thromb. Res. 39*, 49−61.
6. Boskovic, D. S., Giles, A. R., and Nesheim, M. E. (1990) *J. Biol. Chem. 265*, 10497−10505.
7. Chattopadhyay, A., James, H. L., and Fair, D. S. (1992) *J. Biol. Chem. 267*, 12323−12329.
8. Chen, P. S., Jr., Toribara, T. Y., and Warner, H. (1956) *Anal. Chem. 28*, 1756−1758.
9. Comfurius, P., Bevers, E. M., and Zwaal, R. F. (1990) *J. Lipid Res. 31*, 1719−1721.
10. Comfurius, P., and Zwaal, R. F. (1977) *Biochim. Biophys. Acta 488*, 36−42.
11. Cutsforth, G. A., Whitaker, R. N., Hermans, J., and Lentz, B. R. (1989) *Biochemistry 28*, 7453−7461.
12. Dahlback, B. (1980) *J. Clin. Invest. 66*, 583−591.
13. Di Scipio, R. G., Hermodson, M. A., Yates, S. G., and Davie, E. W. (1977) *Biochemistry 16*, 698−706.
14. Husten, E. J., Esmon, C. T., and Johnson, A. E. (1987) *J. Biol. Chem. 262*, 12953−12961.
15. Jesty, J., and Nemerson, Y. (1976) *Methods Enzymol. 45*, 95−107.
16. Jones, M. E., Lentz, B. R., Dombrose, F. A., and Sandberg, H. (1985) *Thromb. Res. 39*, 711−724.
17. Juneja, L. R., Kazuoka, T., Goto, N., Yamane, T., and Shimizu, S. (1989) *Biochim. Biophys. Acta 1003*, 277−283.
18. Koppaka, V., Wang, J., Banerjee, M., and Lentz, B. R. (1996) *Biochemistry 35*, 7482−7491.
19. Majumder, R., Weinreb, G., and Lentz, B. R. (2002) *J. Biol. Chem.* (in review).
20. Pluckthun, A., and Dennis, E. A. (1981) *J. Phys. Chem. 85*, 678−683.
21. Pluckthun, A., and Dennis, E. A. (1982) *Biochemistry 21*, 1743−1750.
22. Sandberg, H., Bode, A. P., Dombrose, F. A., Hoechli, M., and Lentz, B. R. (1985) *Thromb. Res. 39*, 63−79.
23. Sims, P. J., Wiedmer, T., Esmon, C. T., Weiss, H. J., and Shattil, S. J. (1989) *J. Biol. Chem. 264*, 17049−17057.
24. Srivastava, A., Wang, J.-F., Stenflo, J., Rezaie, A. R., Esmon, C. T., and Lentz, B. R. (2002) *J. Biol. Chem. 277*, 1855−1863.
25. Wang, J., Majumder, R., and Lentz, B. R. (2002) *Biophys. J.* (in press).

BI020017P